

Optical and Electrical Characterizations of Ultrathin Films Self-Assembled from 11-Aminoundecanoic Acid Capped TiO₂ Nanoparticles and Polyallylamine Hydrochloride[†]

Thierry Cassagneau,[‡] Janos H. Fendler,^{*,‡} and Thomas E. Mallouk[§]

Center for Advanced Materials Processing, Clarkson University, PO Box 5814, Potsdam, New York 13699-5814, and Department of Chemistry, 152 Davey Laboratory, The Pennsylvania State University, University Park, Pennsylvania 16802

Received June 16, 1999. In Final Form: August 30, 1999

11-Aminoundecanoic acid capped titanium dioxide (capped-TiO₂) nanoparticles (63 ± 2 Å total diameter and 20–24 Å core diameter) and polyallylamine hydrochloride, PAH, have been layer-by-layer self-assembled onto precoated (by poly(diallyldimethylammonium chloride), PDDA, or PAH) substrates. The ultrathin S-PDDA(capped-TiO₂/PAH)_n (n = 5, 10, 15) films have been characterized by absorption and surface plasmon spectroscopies, cyclic voltammetry, and scanning force microscopy. A S-PDDA(capped-TiO₂/PAH)₁₀ film coated by a layer of gold has been shown to function as a Schottky diode.

Introduction

Ultrathin films, prepared by the layer-by-layer self-assembly of oppositely charged nanoparticles and polyelectrolytes, have been demonstrated to function as electroactive devices.¹ The versatility, relative ease of preparation, and the potential for scale-up has rendered self-assembly to be a viable colloid chemical approach for the fabrication of nanostructured devices.²

The established use in photoelectrical energy conversion³ and photocatalysis⁴ has prompted the increasing interest in the preparation of titanium dioxide, TiO₂, nanoparticles and nanoparticulate films.^{5–8} Several ap-

proaches have been developed for generating TiO₂ coatings on electrodes. TiO₂ films have been obtained electrochemically by the anodic oxidation titanium sheets or by the sputtering of titanium, followed by an etching treatment.⁵ A well-known sol–gel chemical approach to produce mesoporous films involves the hydrolysis of titanium tetraisopropoxide.⁶ Annealing these mesoporous films has been shown to lead to the formation of a transparent membrane-like TiO₂ coating.⁷ TiO₂ nanoparticles have been also prepared by the controlled hydrolysis of titanium tetrachloride^{8c,9} or by the arrested hydrolysis of titanium tetraisopropoxide in alcoholic media¹⁰ or titanium butoxide in a mixture of acetylacetone and *p*-toluenesulfonic acid.¹¹

The deposition of TiO₂ building blocks, i.e., nanoparticles, by the layer-by-layer self-assembly or by the Langmuir–Blodgett technique allows a rational control of the structure of the ultrathin semiconducting film formed.¹⁰ Importantly, it is possible to characterize films formed from only a couple of layers of nanoparticles and polyelectrolytes. Indeed, we^{1f} and Alivisatos and co-workers^{1a} have successfully observed rectification behavior in a film self-assembled from three sandwich layers of 1,6-hexanedithiol and CdSe nanoparticles. In the present work we report the construction and characterization of an ultrathin Schottky diode, self-assembled from alternating layers of capped TiO₂ nanoparticles and polyelectrolytes and rationalize its rectifying property by energy level diagrams. We used an amino acid (11-aminoundecanoic acid) as an efficient and versatile capping agent for the TiO₂ nanoparticles and showed that its exposed amine group attracts well polyallylamine hydrochloride, PAH.

Experimental Section

Materials. Titanium tetraisopropoxide, 97%, 11-aminoundecanoic acid, 99%, mercaptoethylamine hydrochloride (MEA), poly(styrene-4-sulfonic acid) sodium salt (PSS), 20% solution in

[†] Part of the Special Issue "Clifford A. Bunton: From Reaction Mechanisms to Association Colloids; Crucial Contributions to Physical Organic Chemistry". Dedicated to Professor C. A. Bunton in recognition for his lifelong creativity.

[‡] Clarkson University.

[§] The Pennsylvania State University.

(1) (a) Colvin, V. L.; Schlamp, M. C.; Alivisatos, A. P. *Nature* **1994**, *370*, 354. (b) Fendler, J. H. *Chem. Mater.* **1996**, *8*, 1616. (c) Feldheim, D. L.; Grabar, K. C.; Natan, M. J.; Mallouk, T. E. *J. Am. Chem. Soc.* **1996**, *118*, 7640. (d) Cassagneau, T.; Fendler, J. H. *Adv. Mater.* **1998**, *10*, 877. (e) Moriguchi, I.; Fendler, J. H. *Chem. Mater.* **1998**, *10*, 2205. (f) Cassagneau, T.; Mallouk, T. E.; Fendler, J. H. *J. Am. Chem. Soc.* **1998**, *120*, 7848. (g) Cassagneau, T.; Fendler, J. H. *J. Phys. Chem. B* **1999**, *103*, 1789.

(2) (a) Mallouk, T. E.; Kim, H.-N.; Ollivier, P. J.; Keller, S. W. Ultrathin Films based on Layered Inorganic Solids. In *Comprehensive Supramolecular Chemistry*; Alberti, G., Bein, T., Eds.; Elsevier Science: Oxford, UK, 1996; Vol. 7, pp 189–218. (b) Liu, J.; Kim, A.; Wang, L. Q.; Palmer, B. J.; Chen, Y. L.; Bruinsma, P.; Bunker, B. C.; Exarhos, G. J.; Graff, G. L.; Rieke, P. C.; Fryxell, G. E.; Virden, J. W.; Tarasevich, B. J.; Chick, L. A. *Adv. Colloid Interface Sci.* **1996**, *69*, 131–180. (c) Decher, G. *Layered Nanoarchitectures via Directed Assembly of Anionic and Cationic Molecules*; In *Comprehensive Supramolecular Chemistry*; Sauvage, J.-P., Hosseini, M. W., Eds.; Elsevier Science: Oxford, U.K., 1996; Vol. 9, pp 507–528.

(3) Tan, M. X.; Laibinis, P. E.; Nguyen, S. T.; Kesselman, J. M.; Stanton, C. E.; Lewis, N. S. *Principles and applications of semiconductor photoelectrochemistry*; Tan, M. X., Laibinis, P. E., Nguyen, S. T., Kesselman, J. M., Stanton, C. E., Lewis, N. S., Eds.; John Wiley & Sons: New York, 1994; Vol. 41, pp 21–144.

(4) (a) Kamat, P. V. *Native and Surface Modified Semiconductor Nanoclusters*; Kamat, P. V., Ed.; John Wiley & Sons: New York, 1997; Vol. 44, pp 273–343. (b) Stafford, U.; Gray, K. A.; Kamat, P. V. *Heterog. Chem. Rev.* **1996**, *3*, 77–104. (c) Heller, A. *Acc. Chem. Res.* **1995**, *28*, 503–508.

(5) (a) Torsi, L.; Zamboni, P. G.; Hillman, R.; Loveday, D. C. *J. Chem. Soc., Faraday Trans.* **1993**, *89*, 3941. (b) Torsi, L.; Sabbatini, L.; Zamboni, P. G. *Adv. Mater.* **1995**, *7*, 417

(6) (a) O'Regan, B.; Grätzel, M. *Nature* **1991**, *353*, 737. (b) Nazeeruddin, M. K.; Kay, A.; Rodicio, I.; Humphry-Baker, R.; Muller, E.; Liska, P.; Vlachopoulos, N.; Grätzel, M. *J. Am. Chem. Soc.* **1993**, *115*, 6382.

(7) Sotomayor, J.; Hoyle, R. W.; Will, G.; Fitzmaurice, D. *J. Mater. Chem.* **1998**, *8*, 105.

(8) Frei, H.; Fitzmaurice, D. J.; Grätzel, M. *Langmuir* **1990**, *6*, 198. (b) Moser, J.; Punchedewa, S.; Infelta, P. P.; Grätzel, M. *Langmuir* **1991**, *7*, 3012. (c) Raj, T.; Tiede, D. M.; Thurnauer, M. C. *J. Non-Cryst. Solids* **1996**, *205–207*, 815.

(9) Kormann, C.; Bahnmann, D. W.; Hoffman, M. R. *J. Phys. Chem.* **1988**, *92*, 5196.

(10) Rizza, R.; Fitzmaurice, D.; Hearne, S.; Hughes, G.; Spoto, G.; Ciliberto, E.; Kerp, H.; Schropp, R. *Chem. Mater.* **1997**, *9*, 2969. (b) Kotov, N. A.; Dékány, I.; Fendler, J. H. *J. Phys. Chem.* **1995**, *99*, 13065.

(11) Scolan, E.; Sanchez, C. *Chem. Mater.* **1998**, *10*, 3217.

water, and poly(diallyldimethylammonium chloride) (PDDA), 20 wt %, were purchased from Aldrich. Polyallylamine hydrochloride (PAH), M_w 60 000 was obtained from Polysciences, Inc. All aqueous solutions were prepared from 10 M Ω cm water, obtained by purifying distilled water through a Millipore Milli-Q membrane filtration system. Soda lime float glass, coated with SiO_x and ITO, with $R < 125 \Omega/\square$ and $> 87\%$ transmission were a gift from Photran. Sn[Sb]O_x (ATO)-coated slides of $R \approx 100 \Omega/\square$ were purchased from Delta Technologies, Ltd. All substrates were cleaned with a piranha solution (75% H₂SO₄/25% H₂O₂) prior to be used for the self-assembly. Additionally, cleaned glass substrates were covered with a 5–10 Å thick Cr layer and 400–500 Å Au layer to be used in surface plasmon spectroscopy (see the next section).

Instruments. Absorption spectra were taken on a Hewlett-Packard 8252A instrument. Cyclic voltammetry was performed with a potentiostat (EG&G Princeton Applied Research, model 273) interfaced with a computer running with Head Start software. Cyclic voltammograms were acquired at room temperature in a 0.1 M NH₄⁺Cl⁻ aqueous solution at a scan rate of 100 mV/s, to avoid any possible degradation and dissolution of the multilayers by organic solvents, with a platinum counter electrode, a saturated calomel electrode (SCE) as reference, while the multilayer-supported antimony tin oxide (ATO)-coated glass constituted the working electrode. Metallic coating (Cr, Au) of glass slides (Fisher) was done by evaporation of the metal source at 10⁻⁶ Torr using an Edwards AUTO306 Vacuum system. A quartz crystal thickness monitor was used for determining the deposition rate and the film thickness. Surface plasmon spectroscopic (SPS) measurements were carried out on a home-constructed instrument. Gold–chromium coated glass slides (10 Å chromium, followed by 400–500 Å gold vacuum evaporated onto one side of a microscope slide) were used as the reflection element. The uncoated side of the slide was brought into optical contact with the base of glass prism ($n = 1.52$) by an index matching oil ($n = 1.518 \pm 0.0005$). A p-polarized 632.8 nm beam of a He–Ne laser (20 mW, Hughes) was directed to the base of the prism which was mounted on a stepping motor driven rotator, capable of varying the angle of incidence, θ , and the direction of a large area silicon detector (Newport, 818-SL) with an angle resolution of 0.01°. Each angular scan was fitted to a theoretical reflection curve, calculated by choosing appropriate one-, two-, and three-layer models and constant refractive indices. A JEOL JEM-1200EXII electron microscope, operating at 120 kV was used to characterize naked and capped TiO₂ nanoparticles. Surface imaging of capped-TiO₂ nanoparticles layered onto PAH was performed by atomic force microscopy (AFM) with a Topometrix Explorer 2000 scanning probe microscope in non-contact mode with standard silicon nitride tips (force constant of 0.12 N/m).

Synthesis of Capped TiO₂ Nanoparticles. Nanosized capped TiO₂ nanoparticles (20–24 Å in diameter) were prepared by the slow hydrolysis of titanium tetraisopropoxide¹⁰ in the presence of an alcoholic solution of 11-aminoundecanoic acid. Typically, 0.6 mL of a 4 × 10⁻³ M 2-propanol solution of titanium tetraisopropoxide was added, under vigorous stirring, to 50 mL of a 4 × 10⁻³ M ethanolic solution of 11-aminoundecanoic acid previously heated to 65 °C for 2 min. After the mixture was stirred for 10 min, 0.50 mL of water was added dropwise under vigorous stirring. Stirring was maintained for an additional 10 min at the same temperature, then the heating was turned off and the stirring was extended to 50 min at ambient temperature. The carboxylic acid moiety of 11-aminoundecanoic acid strongly interacts with the positively charged surface of TiO₂ as the hydrolysis–condensation reaction is taking place; thereby it stabilizes a given size population of the nanoparticles. The outer surface of the amino acid capped TiO₂ particles is enriched by the amine groups of 11-aminoundecanoic acid. The yield of this reaction was very low (0.25%) as the source of titanium was not converted into well-dispersed TiO₂ nanoparticles. Allowing the colloidal suspension to settle for 3 days, separating the precipitate, and centrifuging the supernatant resulted in the formation of a very stable (more than 3 months) colloidal titanium dioxide dispersion used in self-assembly. Attempts to vary the amount of amino acid relative to the titanium tetraisopropoxide did not significantly improve the yield. It should be noted that the

addition of water is essential to obtain reproducible results. Additionally, a similar procedure was used without using amino acid capping molecules, to produce naked TiO₂ nanoparticles of comparable size range for comparative studies (see below).

Self-Assembly Procedures. Capped-TiO₂ nanoparticles were laid down onto the cleaned substrates precoated by a thin layer (20 Å) of poly(diallyldimethylammonium chloride), PDDA. Pre-coating was accomplished by immersing the substrate into a 10⁻³ M aqueous solution of PDDA (at pH = 6.5) for 10 min. A sandwich layer of capped-TiO₂, PAH on a precoated substrate (S-PDDA), S-PDDA(capped-TiO₂/PAH), was self-assembled by the following steps: (i) immersing the precoated substrate into an ethanolic suspension of capped-TiO₂ (4 × 10⁻⁷ M) for 20 h; (ii) washing by absolute ethanol and drying under an Ar stream; (iii) immersing into an aqueous 10⁻³ M PAH (at pH = 7.0) for 20 min; (iv) washing by deionized water followed by drying under an Ar stream. An ultrathin film containing n number of sandwich layers, S-PDDA/(capped-TiO₂/PAH) _{n} , was prepared by repeating steps i–iv n number of times. A schematic of the self-assembly is shown in Figure 1A.

For surface plasmon spectroscopy, gold substrates were prepared by evaporating successively a 5–10 Å thick film of Cr and a 400 Å thick film of gold onto well-cleaned microscopic slides. The substrates were exposed to a 2% (w/v) aqueous solution of 2-mercaptoethylamine hydrochloride, MEA, for 12–15 h, washed by and sonicated in ethanol, and extensively washed with water to provide a 7 ± 1 Å thick layer of coverage (as determined by surface plasmon spectroscopy, see below). Self-assembly onto the Au–MEA substrates was carried out as described above.

Results and Discussion

Microscopic, Adsorption, and Optical Characterizations of the Self-Assembled Films. The size of the titania core of capped-TiO₂ nanoparticles was determined by transmission electron microscopy (TEM) and was found to be 23 ± 3 Å.

The self-assembled S-(capped-TiO₂/PAH) _{n} films were characterized by UV–visible absorption and surface plasmon spectroscopy (Figure 2). A regular growth of the film was observed after the deposition of the two first sandwich layers.

It should be noted that while capped-TiO₂ particles were adsorbed onto a PAH layer, we have not succeeded in adsorbing amino acid capped TiO₂ nanoparticles onto negatively charged S-PDDA/PSS surfaces (PSS = poly(styrene-4-sulfonic acid)). These observations are in accord with the postulate that the adhesion of a PAH layer onto amino acid (AA) capped TiO₂ is likely to originate in sharing a proton between the ammonium cation of PAH and the amine terminal amine group of 11-aminoundecanoic acid used for capping the TiO₂ nanoparticles.

Mercaptoethylamine functionalized gold substrates, Au–MEA, were used for performing surface plasmon spectroscopy experiments. Surface plasmon curves were collected after the self-assembly of each layers PAH and capped-TiO₂ (Figure 3). Capped-TiO₂ nanoparticles were observed to interact slowly with a PAH layer, a minimum dipping time of 20 h was necessary to ensure the full coverage of the substrate. The thickness of a capped-TiO₂/PAH sandwich layer was found to be 67 ± 3 Å; of these 4 ± 1 Å was due to the PAH layer and 63 ± 2 Å for the capped-TiO₂ nanoparticle layer (see Figure 1A). The value determined for the capped-TiO₂ nanoparticle layer suggested that titania cores of about 23 Å were stabilized by a 20 Å thick AA layer, which agrees well with the length of an 11-aminoundecanoic acid molecule (close to 20 Å). Additionally, the surface of a capped-TiO₂ layer deposited onto a mica substrate covered with PAH was imaged by AFM (see Figure 4). It can be seen that the surface was fully covered with capped-TiO₂ nanoparticles, with a thickness PAH/capped-TiO₂ of about 61 Å, in fair agree-

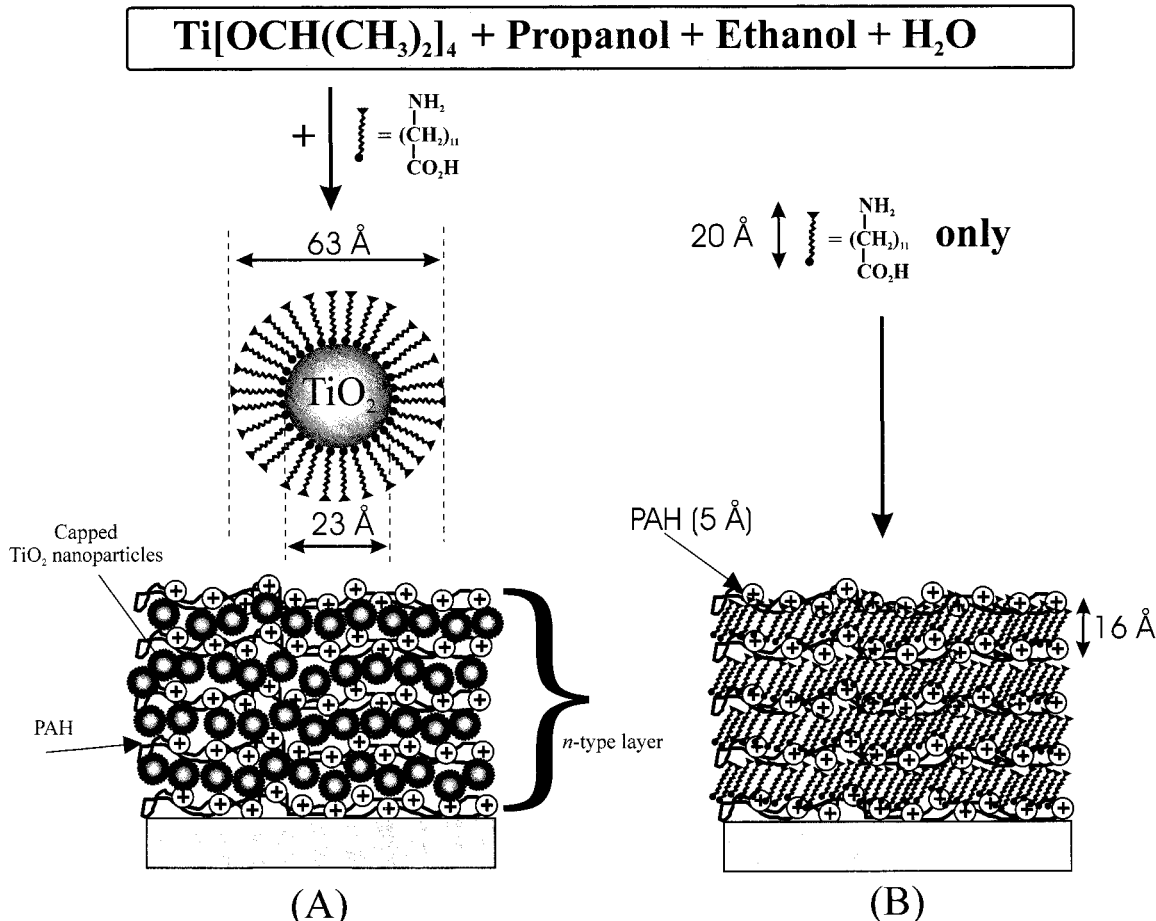


Figure 1. Schematics of the self-assembly of S-PDDA/(AA or capped-TiO₂/PAH)_n film. Titanium isopropoxide is used, in alcoholic medium with a minute amount of water to produce a capped particle in the presence of 11-aminoundecanoic acid (AA). Further layer-by-layer self-assembly is made possible by using PAH as a binder (A). It is also possible to buildup a multilayer composed of AA and PAH (B).

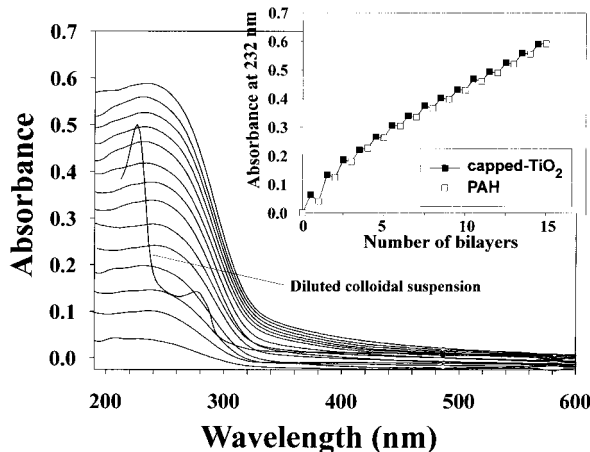


Figure 2. UV-visible absorption spectra of quartz substrates covered with (PAH/capped-TiO₂)_n (where *n* varies from 1 to 10). The insert shows the regular growth of the titania absorption monitored at 232 nm as the number of bilayers PAH/capped-TiO₂ increases.

ment with our expectation (68 Å, 5 Å for PAH and 63 Å for capped-TiO₂ particles).

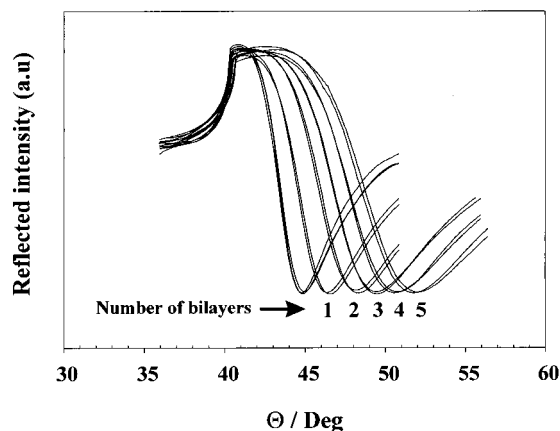
Electrochemical Studies. Cyclic voltammetry was performed using S-PDDA/(capped-TiO₂/PAH)_n films, with *n* = 5, 10, and 15 and S = ATO coated glass, as the working electrode (Figure 5). A regular increase of the charge was observed with the number of sandwich layers self-assembled. Under negative bias, the electrode showed a reversible reduction wave at a potential of -1.13 V vs

SCE (at pH = 7.6), corresponding to a redox level of 3.6 eV below the vacuum level. It is known that strong adsorption of electron-donating surface stabilizers (here AA) shifts the reduction potential of TiO₂ negative. As an n-type semiconductor, TiO₂ is able to reduce species with redox potentials positive of the conduction band edge in the dark.⁸ This property originates in the chelating molecules, which displace the electron-trapping surface energy states, located below the conduction band edge for naked particles, to an energy level in the conduction band.^{8a} The cathodic current began to increase at the flat band potential (estimated to be -0.5 V vs SCE¹²). Integrating the whole redox wave at -1.13 V vs SCE for 10 bilayers and dividing the resulting Coulombic charge by 2 gave a value of 11.7 μC/cm². Assuming that all the titanium atoms were electroactive and that the redox waves accounted for a one-electron process, we found that *N*_{Ti} = 7.28 × 10¹² atoms of Ti per cm² of electrode were laid down for each deposited capped-TiO₂/PAH sandwich layer. By neglecting the polydispersity of the titania colloidal suspension, and assuming particles of spherical shape with a radius *r*_p, one can estimate the "free" surface surrounding each particle in the film from eq 1

$$r_T (\text{\AA}) = 10^{10} \left(\frac{4\rho r_p^3 N_A}{3MN_{Ti}} \right)^{1/2} \quad (1)$$

where *r*_T corresponds to the radius of one nanoparticle

(12) Athanassov, Y.; Rotzinger, F. P.; Péchy, P.; Grätzel, M. *J. Phys. Chem. B* **1997**, *101*, 2558.



Layer	ϵ_r	ϵ_i	d (Å)
Chromium	-30.3456	31.1220	2
Gold	-9.4100	1.1540	369
Mercaptoethylamine (MEA)	2.1740	0.0000	7±1
Poly(allylamine) hydrochloride	2.1800	0.0080	4±1
Capped-TiO ₂ nanoparticles	2.3100	0.0020	63±2

Figure 3. Plasmon resonance curves obtained for the systems Au/mercaptoethylamine (MEA), Au/MEA/polyallylamine hydrochloride (PAH), and Au/MEA/(PAH/capped-TiO₂)_n (with n varying from 1 to 5). The values of the different parameters ϵ_r , ϵ_i , and d (Å) were obtained by a theoretical fit with the experimental results.

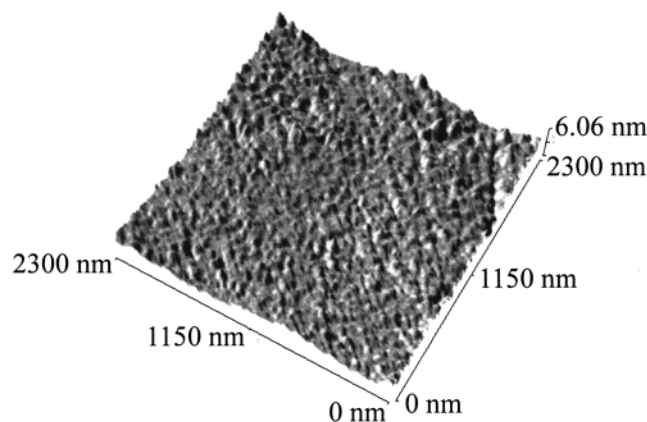


Figure 4. Atomic force microscopy image of one layer of capped-TiO₂ deposited onto a substrate of mica precoated with a thin layer (5 Å) of PAH.

plus the thickness due to the amino acid capping in Å, $\rho = 3.89 \times 10^6 \text{ g m}^{-3}$ is the density of anatase TiO₂, N_A is the Avogadro number, r_p (m) is the radius of the particle without the organic layer (11.5×10^{-10} m), $M = 79.9 \text{ g mol}^{-1}$ is the molecular weight, N_{Ti} is the number of Ti atoms as determined by cyclic voltammetry (CV) per m² of electrode and per layer. Therefore, the formal thickness of the space associated with each nanoparticle can be found by subtracting r_p from r_T . Since the particles were found to have a core diameter of about 23 Å (without the organic layer), one can deduce that each particle should be surrounded by an organic spacer 17.1 Å thick or less, for satisfying the value of N_{Ti} . Despite the approximation of this calculation, there is a good agreement with the value measured by surface plasmon spectroscopy; one would expect about 20 Å in a close packed array, indicating that amino acid chains were slightly intercrossed. It should be

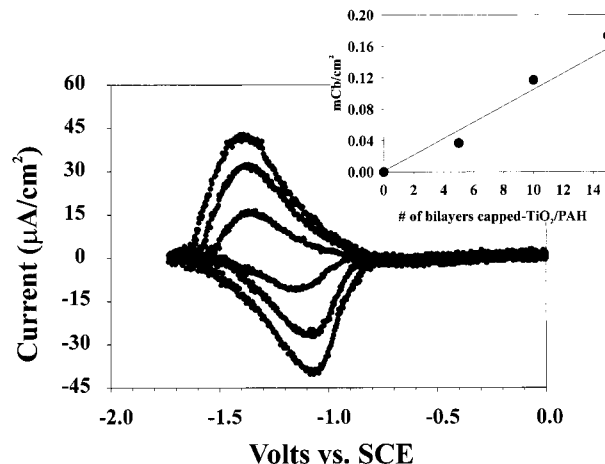


Figure 5. Cyclic voltammograms of ATO/PDDA/(capped-TiO₂/PAH)_n with $n = 5, 10,$ and 15 (corrected for ATO electrode), with a scan rate of 100 mV/s, in 0.1 M NH₄⁺Cl⁻ aqueous solution with a reference calomel electrode. The insert shows the linear increase of the capacity (in mCb/cm²) as a function of the number of sequences capped-TiO₂/PAH.

also noted that in the case of a close-packed array of nanoparticles (hexagonal arrangement) of 63 Å with a titania core of 23 Å in diameter, one expects that 1 cm² should contain 5.44×10^{12} atoms of Ti, this value has to be compared with the N_{Ti} value determined by CV, 7.28×10^{12} atoms of Ti.

These results suggest that one should observe a good coverage of a PAH layer by capped-TiO₂ nanoparticles. To verify this expectation, the surface of one layer of capped-TiO₂ deposited onto PAH was imaged by atomic force microscopy (Figure 4). Not only was the density of particles very high but the total thickness of the film was close to 61 Å (in fair agreement with our expectation, $5 + 63 = 68$ Å). Taking into account the amount of Ti atoms determined by CV, we found the value of the extinction coefficient at 232 nm, ϵ_{232} , to be about $1.4 \times 10^6 \text{ M}^{-1} \text{ cm}^{-1}$ by using the Beer-Lambert law ($d = 63 \times 10^{-8}$ cm is the thickness of one layer of capped-TiO₂ onto PAH and $C[\text{TiO}_2] = 1.92 \times 10^{-2} \text{ M}$ is the concentration of TiO₂ in 1 cm² of that layer, the average optical density determined for one layer was found to be 0.017/cm²).

Interactions between PAH and Capped-TiO₂ Nanoparticles. It is known that PAH can adhere to a gold surface covered by mercaptoethylamine (with its amine groups exposed to the air) while PSS (a negatively charged polyelectrolyte) cannot.^{1f} Since amine groups are neutral, the adhesion is likely due to the sharing of protons at the interface with the mercaptoethylamine layer. Indeed, as -NH₂ groups (from MEA) and ammonium groups (from PAH) are brought together, protons are shared and promote interactions between two layers. This is important in that it conditions the ability of forming a positively charged priming layer onto a gold surface for layer-by-layer self-assembly.

In our approach, we used an amino acid, capable of interacting with the TiO₂ nanoparticle surfaces while exposing the amine groups to the surrounding medium. The interaction between PDDA, PAH, and the amino acid was studied by absorption spectroscopy and surface plasmon spectroscopy. Immersion of a PDDA-coated substrate (S-PDDA) into an aqueous $6 \times 10^{-4} \text{ M}$ solution of 11-aminoundecanoic acid (in the absence of TiO₂) was carried out for 1 h, leading to S-PDDA/AA. Interestingly, a multilayer S-PDDA/(AA/PAH) film could be built up by dipping the substrate alternatively in a 10^{-3} M PAH (for 20 min, rinsing by water and drying under a stream of

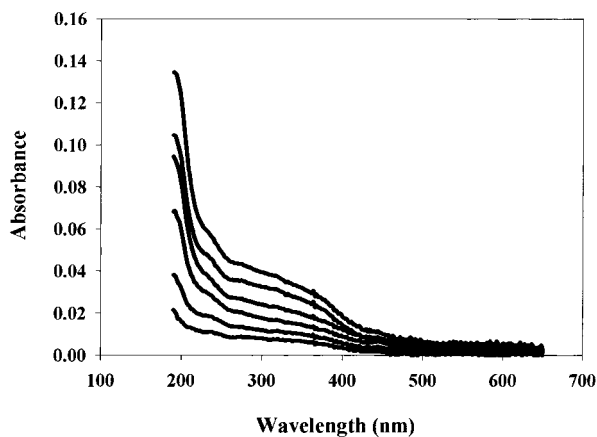


Figure 6. Absorption spectra of bilayers (AA/PAH) consecutively deposited onto a quartz substrate derivatized with a layer of PDDA. Note the regular increase of the absorption with the number of bilayers laid down.

argon) and 6×10^{-4} M AA solution (immersing for 1 h, rinsing by water, and drying under a stream of argon) as indicated by the regular increase of the absorption spectra (Figure 6). Surface plasmon spectroscopy was conducted in parallel, starting with a gold substrate prepared and derivatized with MEA as described above, to determine the typical thickness of an amino acid layer interacting with PDDA or PAH. A value of 16 ± 1 Å was found (with $\epsilon_r = 2.013$ and $\epsilon_i = 0.151$).

It is important to notice that AA was able to interact with PDDA (via carboxyl groups) and PAH (via amine and carboxyl groups). As the substrate with a top layer consisting of PAH was dipped again in an AA solution, the absorption an amino acid layer occurred. Since the PAH was able to interact both with the carboxyl and amine groups, it was possible to buildup a multilayer of amino acid using PAH as a binder (Figure 1B). On the basis of these observations, one would expect the possibility to build up a multilayer from PAH and any building block units functionalized with amine groups. To further study the stability of the interaction responsible for the layering PAH and capped-TiO₂ nanoparticles, films were submitted to different treatments. A film composed of five sequences PAH/capped-TiO₂ (i.e., Au/MEA/(PAH/capped-TiO₂)₅) was contacted with a HCl solution (pH = 2.2). After 2 days, the film collapsed by about 45%, with no further decrease of the thickness with time (within 5 days), as revealed by surface plasmon spectroscopy. Using the approximate value of the extinction coefficient of TiO₂ at 232 nm, we also determined the amount of TiO₂ released into the acidic solution by spectrophotometry. The absorption spectrum corrected for the HCl solution showed a weak absorption band centered at 243 nm (Figure 7). This result demonstrated that increasing the amount of protons inside the multilayers to a value higher than the PAH layers induced the departure of the capped-TiO₂ particles from the film, resulting in a drastic decrease of the total thickness of the film. A simple calculation taking into account the thicknesses of PAH (5 Å), the amino acid (20 Å), and the diameter of the TiO₂ nanoparticle (23 Å), with the value of the measured collapse, indicates that about half of the capping molecules left the film as all the TiO₂ nanoparticles were deintercalated. Importantly, it should be noted that the same experiment carried out under basic conditions (pH = 12) did not lead to a significant collapse of the film after 2 days (only 4%). Using the estimated value of ϵ_{232} , we found that the number of TiO₂ molecules released in the HCl solution was equal to 5.8×10^{13} . This amount corresponded to 8.8×10^{12} atoms of Ti per layer and cm²

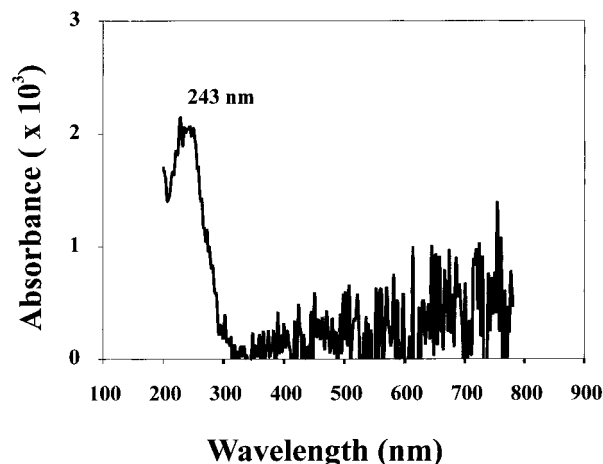


Figure 7. Absorption spectrum of an acidic solution (HCl, pH = 2.2) in which an Au/MEA substrate covered with 10 bilayers PAH/capped-TiO₂ was allowed to stand for 5 days. The absorption band centered at 243 nm was indicative of the presence of TiO₂ deintercalated from the multilayers.

of substrate. This estimate was in a fair agreement with the value obtained from cyclic voltammetry (7.28×10^{12}). These experiments indicated that the interaction between amine/ammonium moieties was relatively insensitive to the pH of the external medium, while this was not the case of the interaction between the carboxyl moieties and the surface of TiO₂ nanoparticles.

Rectification Properties and Energy Level Diagram. It is known that n-type TiO₂ is a strong oxidizer with a valence band edge at 2.6V vs SCE and at pH = 7, and a band gap energy lying between 3 and 3.2 eV. The system ITO/PDDA/(capped-TiO₂/PAH)₁₀/Au exhibited a rectifying branch in the backward direction (ITO(-)/Au(+)) of the *i*-*V* characteristics (Figure 8), obeying the Schottky diode equation:

$$I = I_0 \left[1 - \exp\left(-\frac{qV_{\text{app}}}{nk_B T}\right) \right] \quad (2)$$

where I_0 is the equilibrium exchange current or reverse saturation current, V_{app} corresponds to the applied voltage, k_B is the Boltzmann constant, and T is the temperature in K. By plotting the *i*-*V* curve with a logarithmic current scale, the saturation current was determined to be 2.5 μA. This value, brought into the following equation, allows calculating the barrier height energy between the Fermi level of the metal (Au, 5.4 eV below the vacuum level) and the conduction band edge of TiO₂ nanoparticles

$$I_0 = AR^* T^2 \exp\left(-\frac{q\Phi_b}{k_B T}\right) \quad (3)$$

where A is the active area device (cm²), R^* is the Richardson constant approximated to its free electron value ($120 \text{ A cm}^{-2} \text{ K}^{-2}$), and Φ_b is the barrier potential. It was found that 0.8 eV separated the two energy levels (see Figure 8). On the basis of this value, the electron affinity of the nanoparticles was determined to be 4.40 eV relative to vacuum, in close agreement with the known values (4.30 eV for TiO₂ films, 3.90 eV for TiO₂ nanoparticle films¹²). The band gap energy was deduced from the optical spectrum of a colloidal suspension of capped-TiO₂ by using the following equation, for indirect band gap transitions¹³

$$\alpha h\nu = B(h\nu - E_g)^2 \quad (4)$$

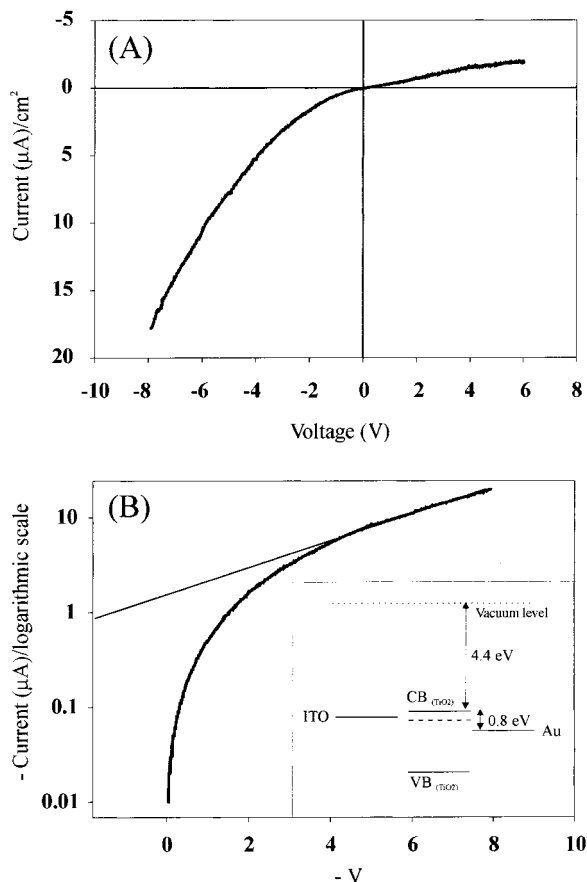


Figure 8. (A) I - V characteristics of the system ITO/PDDA/(capped-TiO₂/PAH)₁₀/Au. (B) Same curve with the current at a logarithmic scale, showing the existence of a linear dependence of $\ln(I)$ vs V as expected for a Schottky junction, the inset shows the energy level diagram of TiO₂ nanoparticles sandwiched between an ITO and Au electrodes.

where α is the absorption coefficient at an energy $h\nu$, B is a constant, $h\nu$ is the energy of the wavelength, and E_g is the band gap energy of the semiconductor. α can be further determined for each wavelength by measuring the optical absorption, A , of a colloidal suspension of stabilized TiO₂ colloids, by means of the relation¹⁴

$$\alpha = \frac{2.303\rho \times 10^3}{lcM} A \quad (5)$$

with $\rho = 3.89 \text{ g cm}^{-3}$ the density of anatase TiO₂, l the optical path length (1 cm), c the molar concentration of TiO₂ ($3.5 \times 10^{-7} \text{ M}$), and M the molecular weight. Plotting

(13) Pankove, J. I. *Optical Processes in Semiconductors*; Dover: New York, 1971; Chapter 3.

(14) Delgass, W. N.; Haller, G. L.; Kellerman, R.; Lundsford, J. In *Spectroscopy in Heterogeneous Catalysis*; Academic Press: New York, 1979; p 128.

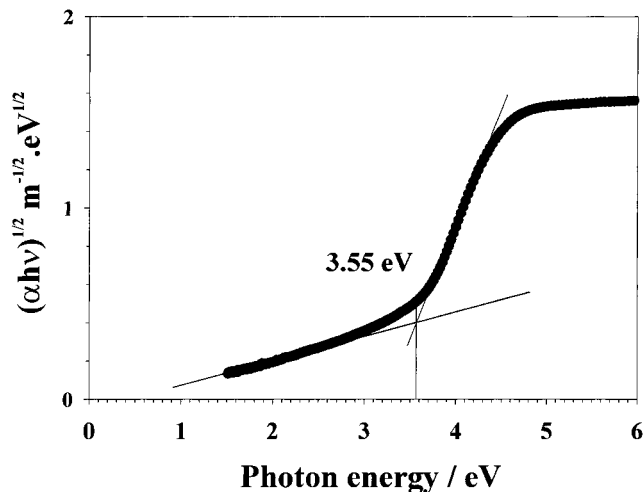


Figure 9. Graphical determination of the optical band gap of capped-TiO₂ nanoparticles.

$\alpha^{1/2}$ vs $\alpha h\nu$ allowed determining a band gap energy value of $3.50 \pm 0.5 \text{ eV}$ (Figure 9). This value was higher than 3.20 eV for bulk anatase, indicating that quantum-size TiO₂ nanoparticles⁹ were incorporated into our systems, as expected from the knowledge of the particle size.

Conclusions

Composite multilayers made of 11-aminoundecanoic acid capped nanoparticles and positively charged polyelectrolytes, PAH, have been prepared by layer-by-layer self-assembly. The multilayers sandwiched between an ITO and Au electrodes exhibited a rectifying behavior, characteristic of a Schottky diode at the junction with the gold lead. Despite the presence of organic spacers (capping molecules and polyelectrolytes) between the arrays of nanoparticles, all titanium dioxide was found to be electroactive for (capped-TiO₂/PAH)_{*n*} films, with $n = 5$ to 15. This approach allowed to sequentially build up *n*-type semiconducting films and is currently exploited in our group to develop rectifying devices based on Ru²⁺(bpy)₃ transition complexes.¹⁵ It should be emphasized that this method of layering can be potentially extended to any oxide particles capable of interacting with the carboxyl groups of any amino acid.

Acknowledgment. We thank the National Science Foundation (CHE-9529202), the New York State Science and Technology Foundation, and Clarkson University's Center for Advanced Materials Processing (CAMP) for support of this research.

LA990776H

(15) Cassagneau, T.; Fendler, J. H.; Johnson, S. A.; Mallouk, T. E. Submitted.